

Bulges *versus* disks: the evolution of angular momentum in cosmological simulations of galaxy formation

Jesus Zavala^{1*}, Takashi Okamoto², Carlos S. Frenk²

¹*Instituto de Ciencias Nucleares, Universidad Nacional Autónoma de México A.P. 70-543, México 04510 D.F., México*

²*Institute for Computational Cosmology, Department of Physics, Durham University, South Road, Durham, DH1 3LE*

Accepted —. Received —; in original form —

ABSTRACT

We investigate the evolution of angular momentum in simulations of galaxy formation in a cold dark matter universe. We analyse two model galaxies produced in the N-body/hydrodynamic simulations of Okamoto et al. Starting from identical initial conditions, but using different assumptions for the baryonic physics, one of the simulations produced a bulge-dominated galaxy and the other one a disk-dominated galaxy. The main difference is the treatment of star formation and feedback, both of which were designed to be more efficient in the disk-dominated object. We find that the specific angular momentum of the disk-dominated galaxy tracks the evolution of the angular momentum of the dark matter halo very closely: the angular momentum grows as predicted by linear theory until the epoch of maximum expansion and remains constant thereafter. By contrast, the evolution of the angular momentum of the bulge-dominated galaxy resembles that of the central, most bound halo material: it also grows at first according to linear theory, but 90% of it is rapidly lost as pre-galactic fragments, into which gas had cooled efficiently, merge, transferring their orbital angular momentum to the outer halo by tidal effects. The disk-dominated galaxy avoids this fate because the strong feedback reheats the gas which accumulates in an extended hot reservoir and only begins to cool once the merging activity has subsided. Our analysis lends strong support to the classical theory of disk formation whereby tidally torqued gas is accreted into the centre of the halo conserving its angular momentum.

Key words: methods: numerical – galaxies: evolution – galaxies: formation

1 INTRODUCTION

In the standard theory of galaxy formation in the cold dark matter (CDM) cosmogony, disk galaxies form when rotating gas cools inside a dark matter halo and fragments into stars. Analytic and semi-analytic calculations of this process start by assuming that tidal torques at early times impart the same specific angular momentum to the gas and the halo and that the angular momentum of the gas is conserved during the collapse (Fall & Efstathiou 1980; Mo et al. 1998; Cole et al. 2000). It is unclear whether this assumption holds in gasdynamic simulations of galaxy formation.

The first attempts to simulate the formation of a spiral galaxy from cold dark matter initial conditions generally failed, producing objects with overly centrally concentrated distributions of gas and stars. It became immediately apparent that the root cause of this problem was a net transfer of angular momentum from the baryons to the dark matter halo during the aggregation of the galaxy through mergers (Navarro & Benz 1991; Navarro & White 1994;

Navarro, Frenk, & White 1995). This is known as the “angular momentum problem”. It was suspected from the start that its solution was likely to involve feedback processes that would regulate the supply of gas to the galaxy.

More recent simulations within the CDM framework have produced more promising disk galaxies. Thacker & Couchman (2001) obtained a reasonably realistic disk by assuming that gas cooling is strongly suppressed by feedback effects. Their simulation, however, stopped at $z = 0.5$. Steinmetz & Navarro (2002), using different prescriptions for star formation and feedback, found that a broad range of galaxy morphologies could be produced. In related work, Abadi et al. (2003) obtained a disk galaxy with a realistic density profile but not enough angular momentum. Sommer-Larsen, Götz, & Portinari (2003) were also able to generate a variety of morphological types, including disks, by assuming strong feedback at high redshift to prevent the early collapse of baryons. Their disks, however, also rotated about a factor of 2 too slowly. On the other hand, Governato et al. (2004) produced a disk galaxy without requiring strong feedback and ascribed the angular momentum problem to a lack of numerical resolution. However, subsequently, Governato et al. (2007) were forced to in-

* Present address: Shanghai Astronomical Observatory, Nandan Road 80, Shanghai 200030, China; jzavala@shao.ac.cn

voked strong feedback in order to match the Tully-Fisher relation. Robertson et al. (2004) adopted a multiphase model for the star-forming interstellar medium (ISM) which stabilises gaseous disks against the Toomre instability, and produced a galaxy with an exponential surface brightness profile but insufficient angular momentum in the inner parts. They concluded that the fragmentation of gaseous disks caused by the Toomre instability is the main cause of the angular momentum loss in simulations that usually assume an isothermal ISM at a temperature of $\sim 10^4$ K.

Okamoto et al. (2005) also assumed a multiphase model for the ISM and a top-heavy initial mass function (IMF) for stars formed in starbursts, as required for the semi-analytic model of Baugh et al. (2005) to match the number counts of bright submillimeter galaxies. By varying the criteria for starbursts in their simulations, Okamoto et al. (2005) were able to produce galaxies with a variety of morphological types, from ellipticals to spirals, starting from exactly the same initial conditions. They showed that disk galaxies can form in halos that have a relatively quiet merger history if the early collapse of baryons is inhibited by strong feedback, in this case generated by the evolution of a stellar population with a top-heavy IMF.

In this *Letter*, we analyse two of the galaxies simulated by Okamoto et al. (2005), one which ended up as a bulge-dominated galaxy and another that formed an extended stellar disk. We trace the time evolution of the angular momentum of the dark matter and the gas, and we distinguish between the evolution of the inner part of the dark halo and the halo as a whole. We show explicitly that mergers transfer angular momentum from the inner parts of the system to the outer halo. This process is one aspect of the redistribution of angular momentum during virialization investigated in N-body simulations by D’Onghia & Navarro (2007). Thus, the spin of the *central* part of the final system contains a fossil record of the merger history of the object.

This *Letter* is organised as follows. The simulations are briefly described in Section 2. The method we use to follow the angular momentum of the different components is explained in Section 3 where we also present our results. We conclude in section 4.

2 THE SIMULATIONS

Details of the simulations that we analyse here may be found in Okamoto et al. (2005). The initial conditions were extracted from a cosmological N-body simulation (of a cubical region of side $35.325h^{-1}$ Mpc) and correspond to a dark matter halo of present day virial mass $M_{\text{vir}} \simeq 1.2 \times 10^{12} h^{-1} M_{\odot}$ which has a quiet merging history since $z \sim 1$. The simulations were carried out using the N-body/SPH code GADGET-2 (Springel 2005). They include a multiphase description of the star-forming gas and make use of the ‘phase-decoupling’ technique introduced by Okamoto et al. (2003) to suppress the spurious angular momentum transfer from cold disk gas to ambient hot halo gas which would otherwise arise from the very nature of SPH.

One of the two simulations that we analyse is the “no-burst” model which has a standard prescription for star formation, tuned to reproduce the local Kennicutt (1998) relation between star formation rate and gas density. This simulation yielded a galaxy with a large bulge and a small disk, to which we will henceforth refer as the “bulge-dominated” galaxy (left panels in Fig. 1).

The second simulation is the “shock-burst” model in which the star formation efficiency is higher than average in gas that has recently been shock-heated. The stellar populations that form from

this gas in a starburst are assumed to have a top-heavy IMF. Thus, in this model there is additional supernova heating available when galaxies merge. The outcome of this simulation was a galaxy with a large disk and a small bulge – the “disk-dominated” galaxy (right panels in Fig. 1). Interestingly, the satellites of the main galaxy in this model provide a good match to the properties of the Milky Way satellites (Libeskind et al. 2007).

Okamoto et al. (2005) presented a third simulation in their paper, the “density-burst” model, which led also to a bulge-dominated object. We do not discuss our analysis of this object in this *Letter* because this galaxy lost most of its baryons in strong galactic winds and is therefore not particularly suitable for studying the evolution of the angular momentum of the baryonic component. Nevertheless, we have checked that the results for this object are qualitatively similar to those of the “bulge-dominated” galaxy.

In our analysis of angular momentum evolution, we distinguish three (Lagrangian) components for each galaxy at $z = 0$. The centre of the system is taken to be the density peak of the stellar distribution. The first component is the dark matter halo which we define as the dark matter mass contained within the virial radius, r_v . We take r_v to be the radius within which the mean density is 100 times the critical value (Eke, Navarro, & Frenk 1998). For both galaxies, the halo mass is $\sim 10^{12} h^{-1} M_{\odot}$ and the virial radius is $\sim 210 h^{-1}$ kpc. The second component we consider is the *inner Lagrangian halo* which we define as the 10% most bound dark matter particles at redshift $z = 0$. The third component is the “galaxy” which we define as the stars and dense gas ($\rho \geq 7 \times 10^{-27} \text{ g cm}^{-3}$) contained within $0.1r_v$. In the next section, we will follow the evolution of these three components.

Fig. 1 shows edge-on and face-on views of the surface density of the two galaxies. The bulge-dominated galaxy (left) has a centrally concentrated spheroidal bulge, a small disk and an extended, nearly spherical stellar halo. The disk-dominated galaxy (right) has a small central bulge, an extended disk and a spheroidal stellar halo.

3 RESULTS

We now calculate the evolution of the physical (i.e. not the comoving) angular momentum of the particles that make up each of the three components defined in Section 2 at the present day: the total halo, the inner halo and the galaxy. We identify the same particles at each output time in the simulation, find the position and velocity of their centre of mass and compute the physical angular momentum of each system, L_T , as

$$L_T = \sum_i \mathbf{l}_i = \sum_i m_i (\mathbf{r}_i \times \mathbf{v}_i), \quad (1)$$

where \mathbf{r}_i and \mathbf{v}_i denote, respectively, the position and velocity of particle i relative to the centre of mass of the system. The total specific angular momentum, \mathbf{L} , is given by $\mathbf{L} = \mathbf{L}_T / M_T$, where M_T is the total mass of the system.

3.1 Dark matter component

First, we focus in the dark matter component. The evolution of the baryons has only a minor effect on the evolution of the halo and so the results are very similar for the bulge- and disk-dominated galaxies. We show results only for the latter case.

The top-left panel of Fig. 2 shows the evolution of the physical *rms* radius of the dark matter halo as a function of the scale factor, normalised to the present day *rms* radius. The evolution closely

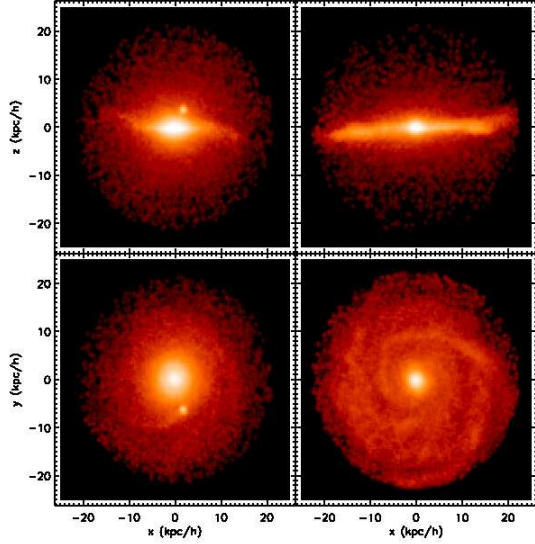


Figure 1. Edge-on (top) and face-on (bottom) views of the baryonic component of the bulge-dominated (left) and disk-dominated (right) galaxies. Stars and gas with $\rho_g \geq 7 \times 10^{-27} \text{ gr cm}^{-3}$ within 10% of the virial radius make up the baryonic component. The brightness indicates the projected mass density.

follows the spherical collapse model: the system expands, reaches a maximum radius at $1+z \sim 3$ and begins to collapse at $1+z \sim 2$ to form a virialised system of size about half the radius at maximum expansion. The middle-left panel shows the evolution of the magnitude of the specific angular momentum, $L = |L|$, for all the dark matter particles that lie within r_v at $z = 0$ as a function of a , once again normalised to the present day value. During the rapidly expanding phase, ($1+z > 4$), the system gains angular momentum in proportion to $a^{3/2}$, as first calculated from tidal torque theory by White (1984). During the collapsing phase, ($1+z < 2$), the magnitude of the angular momentum remains nearly constant. To show the dependence on the scale factor more clearly, in the bottom-left panel of the figure we scale the specific angular momentum by $a^{3/2}$. This plot clearly shows the two distinct evolutionary phases, indicated by the dashed ($L \propto a^{3/2}$) and dotted ($L = \text{const.}$) lines. Our results agree well with previous analyzes of N-body simulations (e.g. White 1984; Catelan & Theuns 1996).

The right panels of Figure 2 show the same quantities as the left panels but now for the particles that make up the inner dark matter halo (i.e. the 10% most bound mass) at $z = 0$. Since this subsystem has a higher overdensity than the halo as a whole, it reaches maximum expansion earlier and begins to collapse at $1+z \sim 5$. The inner halo shrinks more rapidly than the halo as a whole and ends up with a radius that is only about 1/5 of the size at maximum expansion. At $1+z \sim 5$, the particles that will end up in the inner halo are not contained in a single object, but in several subclumps which subsequently merge. This is illustrated in Fig. 3 which shows the spatial distribution of the inner halo particles at $1+z \simeq 4$ and 3.3. Many of the fragments merge between these two epochs and it is these mergers that determine the evolution of the r_{rms} size of the system during this period.

The middle and bottom panels of Fig. 2 show that the evolution of the specific angular momentum of the inner halo is very different from that of the halo as a whole. Initially, during the expansion phase, the system gains angular momentum in much the

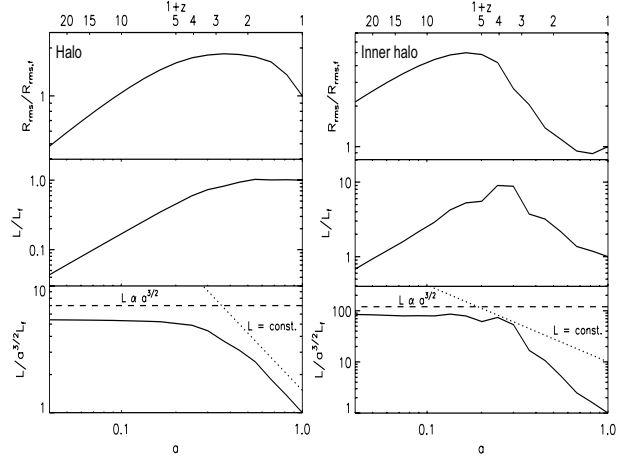


Figure 2. Left: the evolution of the r_{rms} radius (top panel) and the specific angular momentum (middle and bottom panels) of the dark matter particles that lie within r_v at $z = 0$. In the bottom panel the dashed line indicates $L \propto a^{3/2}$ and the dotted line $L = \text{const.}$ Right: as the left but for the particles that make the inner dark matter halo as defined in Section 2. All physical quantities are normalized to their values at the present day.

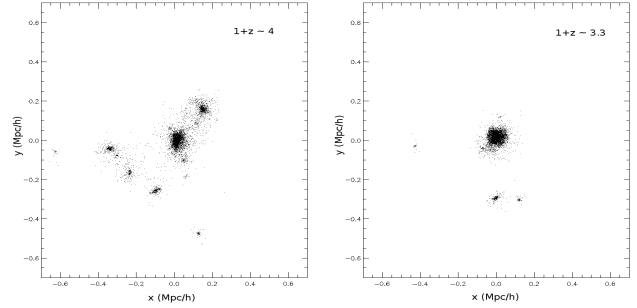


Figure 3. Projected positions of the dark matter particles which will eventually end up in the inner halo at $z = 0$. The left panel shows the distribution at $1+z \sim 4$ and the right panel at $1+z \sim 3.3$.

same way as the halo as a whole, roughly following the $L \propto a^{3/2}$ scaling. However, after maximum expansion, ($1+z < 4$), the inner halo rapidly loses most of its angular momentum. This behaviour is due to the intense merging activity illustrated in Fig. 3. As fragments are drawn towards the centre by dynamical friction, the asymmetric distribution of dark matter produced by gravitational tides exerts a torque which transfers the orbital angular momentum of the fragments to the outer halo. Each merger event is accompanied by a decline in the angular momentum and in this way, the angular momentum is drained from the inner halo. During this phase, the angular momentum of this system declines roughly as a^{-3} . This behaviour was first noted in the early cold dark matter simulations of Frenk et al. (1985). The redistribution of angular momentum during virialization has been studied in detail by D'Onghia & Navarro (2007).

3.2 Bulge-dominated galaxy

We now perform the same analysis on the baryonic component of the bulge-dominated galaxy illustrated in the left panels of Fig. 1. The total stellar mass of this system is $6.75 \times 10^{10} h^{-1} M_\odot$ and the total gas mass is $7.5 \times 10^9 h^{-1} M_\odot$.

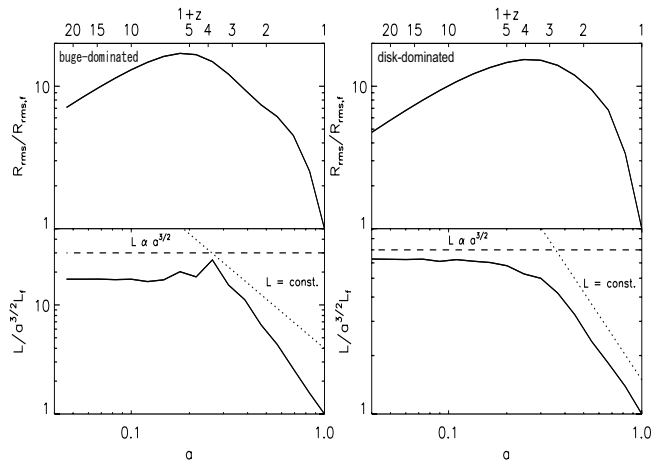


Figure 4. Evolution of the *rms* radius (upper panel) and specific angular momentum evolution (lower panel) with scale factor for the baryonic component. The left panels correspond to the bulge-dominated galaxy and the right panels to the disk-dominated galaxy.

The evolution of the *rms* radius of this galaxy, plotted in the upper-left panel of Fig. 4, is remarkably similar to that of the inner dark matter halo. The system expands until $1+z \sim 5$ and then collapses. The evolution of the magnitude of the specific angular momentum (lower-left panel) is also very similar to that of the inner dark matter halo. During the expanding phase, the system gains angular momentum in proportion to $a^{3/2}$, as expected from linear theory. After $1+z \simeq 4$, the system rapidly loses its angular momentum, just as the inner dark matter halo did, transferring it to the outer halo. The decline in the specific angular momentum of the galaxy during the collapsing phase is less abrupt than for the inner halo, scaling roughly a $L \propto a^{-1}$.

The similarity in the behaviour of the bulge-dominated galaxy and the inner halo arises because even before the collapse phase, the cold baryonic material is distributed in a similar way to the mass of the inner halo. Radiative cooling of gas is very efficient in dense subclumps at early times and, in this simulation, much of the gas cools and turns into stars inside the fragments that will later merge to make the inner halo. Very little gas is left over for later accretion. Just as in the dark matter only case, the fragments, now containing a mixture of dark matter and cold baryons (stars and dense gas), merge together transferring their orbital angular momentum to the outer halo. With most of the final cold baryons already in place within the fragments at early times, the end result of the collapse and merger phase is a bulge-dominated object.

3.3 Disk-dominated galaxy

We now analyse the disk-dominated galaxy illustrated in the right-hand panels of Fig. 1. This galaxy has $4.17 \times 10^{10} h^{-1} M_{\odot}$ in stars and $1.53 \times 10^{10} h^{-1} M_{\odot}$ in dense gas. The results are shown in the right hand panels of Fig. 4.

The top-right panel of Fig. 4 shows that the baryonic material that will end up in the galaxy expands until $1+z \simeq 4$ and then begins to collapse. This happens slightly earlier than for the bulge-dominated galaxy. The lower-right panel shows that, as for all other objects and components, the evolution of the angular momentum during the expanding phase follows linear theory closely, with $L \propto a^{3/2}$. However, unlike the bulge-dominated galaxy, the angular momentum of the system remains nearly constant during

the collapsing phase ($1+z < 3$), indicating that the accreting gas conserves its angular momentum. This behaviour is reminiscent of that of the halo as a whole, illustrated in Fig. 2. Indeed, the lower-right panel of Figs. 4 is very similar to the bottom-left panel of Fig 2.

The correspondence between the evolution of the angular momentum of the baryonic material of the disk-dominated galaxy and of the material that makes up the halo follows from the similarity of their spatial distributions at the time of maximum expansion. As discussed in Section 2, mergers of subclumps in this simulation induce large-scale shocks in the gas which result in an increased star formation efficiency. This, in turn, produces strong feedback which is further promoted by the assumed top-heavy starburst IMF, keeping the gas out of the merging fragments. Since the merger rate is higher at high redshift, this strong feedback suppresses the early collapse of gas into small proto-galaxies. The vast majority of the baryons that will make up the final galaxy become decoupled from the sub-clumps and accumulate in a hot gas reservoir in the main halo. This hot gas has similar specific angular momentum to the halo and, as it loses its pressure support through radiative cooling, it accretes onto the galaxy conserving its angular momentum. The key to the formation of disk galaxies is hence the suppression of the early collapse of baryons into merging fragments, as anticipated by many authors (Navarro & Steinmetz 2000; Okamoto et al. 2005; Sommer-Larsen & Dolgov 2001; Thacker & Couchman 2001; Weil, Eke, & Efstathiou 1998).

Finally, in Fig. 5 we show the evolution of the unnormalised specific angular momentum of the whole halo (solid line) and of the baryonic components of both galaxies, the bulge-dominated (dashed line) and the disk-dominated (dotted line) objects. This figure indicates that it is not only the shape of the time dependence of the angular momentum that is similar between the halo and the baryons of the disk-dominated galaxy, but, remarkably, also the value of the specific angular momentum of the two components. Thus, our simulation provides strong support for the classical theory of disk formation whereby tidally torqued gas is accreted into the centre of the halo conserving its angular momentum (Fall & Efstathiou 1980; Mo et al. 1998). This is the assumption made in semi-analytic models of galaxy formation (e.g. Cole et al. 2000). By contrast, the bulge-dominated galaxy ends up with only about 20% of the specific angular momentum of its halo.

4 DISCUSSION AND CONCLUSIONS

The series of N-body/SPH simulations of galaxy formation in a cold dark matter universe carried out by Okamoto et al. (2005) led to the puzzling result that galaxies with very different morphologies can form in the same dark matter halo depending on the details of the assumed star formation and feedback prescriptions. In this letter, we have investigated the evolution of the specific angular momentum as a possible explanation for why relatively small differences in the assumed baryonic processes can result in such different outcomes. We have analyzed the bulge-dominated and the disk-dominated galaxies simulated (from identical initial conditions) by Okamoto et al. (2005). We trace back all the dark matter particles that end up within the virial radius of the halo (r_v), as well as those that end up in the central parts of the halo by virtue of being in the top 10 percentile of the binding energy distribution. We also trace back the baryonic particles that end up as a galaxy, i.e. as cold baryons (star particles and dense gas) within 10% of r_v at $z = 0$.

The angular momentum of the dark matter halo evolves al-

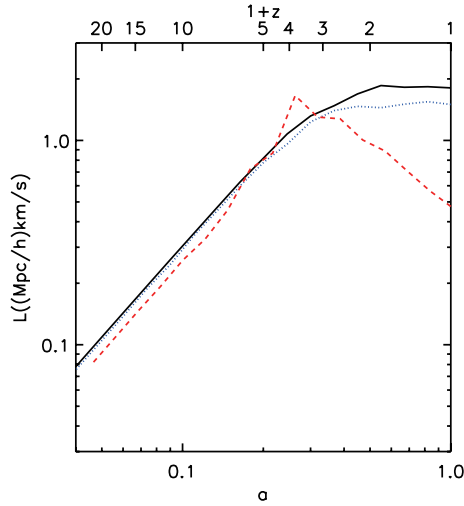


Figure 5. Specific angular momentum of the dark matter component (solid line) and of the baryonic component of the bluge-dominated galaxy (dashed line) and of the disk-dominated galaxy (dotted line).

most identically in the two simulations. The specific angular momentum of the halo as a whole grows initially as predicted by tidal torque theory in the linear regime, in proportion to $a^{3/2}$ (White 1984; Catelan & Theuns 1996). This phase lasts until maximum expansion is reached. Thereafter, the angular momentum of the dark matter remains constant, as the system collapses to a virialized configuration. By contrast, the evolution of the most bound 10% of the dark matter is strikingly different. In the linear phase this material behaves just as the halo as a whole but, after maximum expansion, its specific angular momentum rapidly declines to $\sim 10\%$ of its maximum value. The decline occurs in episodes associated with the mergers that build up the central halo. Most of the angular momentum of these fragments is invested in their orbits and is transferred to the outer halo by tidal forces as the fragments sink by dynamical friction.

The baryonic component evolves very differently in the two simulations. In essence, in the disk-dominated galaxy, the specific angular momentum of the baryons tracks that of the halo as a whole, while in the bulge-dominated galaxy, it tracks the evolution of the central halo material. The reason for the difference can be traced back to the different strengths of feedback in the two galaxies at early times. In the bulge-dominated galaxy, feedback is weak and most of the baryons rapidly cool and condense into stars within sub-galactic fragments. As these halo fragments merge and give up their angular momentum to the outer halo, so do the baryon clumps within them. The result is a slowly-rotating central bulge. A small amount of residual gas rains in later on forming a small disk. In the disk-dominated galaxy, by contrast, feedback is strong at early times, the gas is reheated before it can make a substantial mass of stars and, instead, accumulates in an extended hot reservoir which acquires a specific angular momentum similar to that of the dark halo. By the time this gas is able to cool, much of the merger activity has subsided and so the gas is able to dissipate and collapse into an centrifugally supported disk configuration conserving its angular momentum. Not only does the angular momentum of the baryonic material track the evolution of the angular momentum of the halo, but the actual values of the specific angular momentum of both components are very similar throughout the entire history of the galaxy. By contrast, the specific angular momentum of the bulge-dominated galaxy is only about 20% of the halo value.

Our results indicate that the key to the formation of disk galaxies in the cold dark matter cosmology is the suppression of the early collapse of baryons into small, dense halos. Decoupled from the sub-halos that are destined to merge, the baryons (which at this time are mostly gas) are tidally torqued just as their host halo and gain the same amount of specific angular momentum. Our results thus provide strong support for the classical theory of disk formation by Fall & Efstathiou (1980) and Mo et al. (1998).

ACKNOWLEDGMENTS

This work was carried out during a research visit of JZ to the ICC at Durham supported by the EU's ALFA programme through the Latin American European Network for Astrophysics and Cosmology. JZ acknowledges support from CONACyT and DGEP-UNAM scholarships. We thank Simon White for insightful comments. TO and CSF acknowledge support from PPARC. CSF acknowledges receipt of the Royal Society Wolfson Research Merit Award. The simulations were carried out at the Cosmology Machine at the ICC.

REFERENCES

- Abadi M. G., Navarro J. F., Steinmetz M., Eke V. R., 2003, *ApJ*, 591, 499
- Baugh, C. M., Lacey, C. G., Frenk, C. S., Granato, G. L., Silva, L., Bressan, A., Benson, A. J., & Cole, S. 2005, *MNRAS*, 356, 1191
- Catelan P., Theuns T., 1996, *MNRAS*, 282, 436
- Cole, S., Lacey, C. G., Baugh, C. M., & Frenk, C. S. 2000, *MNRAS*, 319, 168
- Eke V. R., Navarro J. F., Frenk C. S., 1998, *ApJ*, 503, 569
- D'Onghia E., Navarro J. F., 2007, *MNRAS*, 380, L58
- Fall S. M., Efstathiou G., 1980, *MNRAS*, 193, 189
- Frenk, C. S., White, S. D. M., Efstathiou, G., & Davis, M. 1985, *Nature*, 317, 595
- Governato F., et al., 2004, *ApJ*, 607, 688
- Governato F., Willman B., Mayer L., Brooks A., Stinson G., Valenzuela O., Wadsley J., Quinn T., 2007, *MNRAS*, 374, 1479
- Kennicutt R. C., Jr., 1998, *ApJ*, 498, 541
- Libeskind N. I., Cole S., Frenk C. S., Okamoto T., Jenkins A., 2007, *MNRAS*, 374, 16
- Mo, H. J., Mao, S., & White, S. D. M. 1998, *MNRAS*, 295, 319
- Navarro J. F., Benz W., 1991, *ApJ*, 380, 320
- Navarro J. F., Frenk C. S., White S. D. M., 1995, *MNRAS*, 275, 56
- Navarro J. F., White S. D. M., 1994, *MNRAS*, 267, 401
- Navarro J. F., Steinmetz M., 2000, *ApJ*, 538, 477
- Okamoto T., Eke V. R., Frenk C. S., Jenkins A., 2005, *MNRAS*, 363, 1299
- Okamoto T., Jenkins A., Eke V. R., Quilis V., Frenk C. S., 2003, *MNRAS*, 345, 429
- Robertson B., Yoshida N., Springel V., Hernquist L., 2004, *ApJ*, 606, 32
- Sommer-Larsen J., Dolgov A., 2001, *ApJ*, 551, 608
- Sommer-Larsen J., Götz M., Portinari L., 2003, *ApJ*, 596, 47
- Springel, V. 2005, *MNRAS*, 364, 1105
- Steinmetz M., Navarro J. F., 2002, *NewA*, 7, 155
- Thacker R. J., Couchman H. M. P., 2001, *ApJ*, 555, L17
- Weil M. L., Eke V. R., Efstathiou G., 1998, *MNRAS*, 300, 773
- White S. D. M., 1984, *ApJ*, 286, 38

This paper has been typeset from a $\text{T}_{\text{E}}\text{X}/\text{L}^{\text{A}}\text{T}_{\text{E}}\text{X}$ file prepared by the author.